Journal of Phytology 2026, 18: 14-24
https://doi.org/10.25081/jp.2026.v18.9911

Research Article

Antibiofilm and antimicrobial activity studies of the essential oil, extract, and green synthesized silver nanoparticles from the leaves of *Syzygium stocksii*

B. S. Devika[1], J. Devi[2], P. Biju[3], Praveen Kumar[2], P. S. Hema[4], G. Ajayakumar[1]*

[1]*Department of Chemistry, Government College for Women, Thiruvananthapuram-695014, Kerala, India*
[2]*Department of Zoology, Government College for Women, Thiruvananthapuram-695014, Kerala, India*
[3]*Department of Botany, Government College Kasaragod, Kasaragod-671123, Kerala, India*
[4]*Department of Chemistry, HHMSPB NSS College for Women, Neeramankara, Thiruvananthapuram-695040, Kerala, India*

(Received: September 30, 2025; Revised: February 14, 2026; Accepted: March 03, 2026; Published: March 20, 2026)

*Corresponding author: G. Ajayakumar, E-mail: ajayakumar@gcwtvm.ac.in

Abstract

This study investigates the phytochemical composition and biological potential of the leaves of *Syzygium stocksii*. For the first time, the presence of β-Ocimenes (E and Z isomers) was identified in the leaf extracts. The total phenolic and flavonoid contents were quantified, and the extracts demonstrated notable antioxidant activity. The ethanolic extract was further applied in the green synthesis of silver nanoparticles (AgNPs), which were evaluated for their antimicrobial and antibiofilm properties. Antimicrobial assays were performed against *Acinetobacter baumannii, Pseudomonas aeruginosa, Bacillus cereus, Streptococcus mutans,* and *Candida albicans*, revealing *S. mutans* and *A. baumannii* as the most sensitive to the essential oils. Importantly, the AgNPs exhibited strong antibiofilm activity against *P. aeruginosa*. These findings not only broaden the phytochemical profile of *S. stocksii* but also highlight its potential as a source of natural antioxidants, antimicrobials, and eco-friendly nanomaterials with promising biomedical applications.

Keywords: *Syzygium stocksii*, Ocimene, Silver nanoparticles, Antimicrobial activity, Antibiofilm activity

Introduction

Plant Secondary Metabolites (PSMs), non-essential compounds produced by plants known as phytochemicals, have been extensively explored for their medicinal applications (Siddiqui & Prasad, 2016). Curcumin from *Curcuma longa*, for instance, has been reported to have potential in treating COVID-19 because of its antiviral and anti-inflammatory effects (Babaei *et al.,* 2020). Plant-derived essential oils (EOs), which are rich in secondary metabolites and traditionally used in aromatherapy, possess strong antimicrobial properties (Amorati *et al.,* 2013). The global rise in antibiotic-resistant bacteria, responsible for over 1.2 million deaths in 2019 (Antimicrobial Resistance Collaborators, 2022), highlights the urgent need for new treatments for bacterial infections. Plant-derived antimicrobials (PDAms) offer a promising alternative, as they often do not result in bacterial resistance (Lewis & Ausubel, 2006). Formulations such as polytoxinol (Simões *et al.,* 2009), containing EOs from *Eucalyptus* and *Melaleuca*, are highly effective against bacteria. Biofilms, bacterial communities on medical implants, are linked to 80% of chronic infections (Cascioferro *et al.,* 2021). Phytochemicals combat microbes by inhibiting their virulence factors and biofilm formation (Slavin *et al.,* 2017). Metal nanoparticles, such as silver nanoparticles (AgNPs), combined with natural products, show promise for penetrating biofilms and combating resistant bacteria (Qayyum & Khan, 2016). In this context, the present study focuses on *S. stocksii*, an endangered species from Southwest India, to explore its phytochemical profile and evaluate its potential as a source of novel plant-derived antimicrobials against resistant bacterial pathogens.

The genus *Syzygium* is included in the myrtle family *Myrtaceae,* which consists of approximately 1200-1800 species distributed worldwide (Ahmad *et al.,* 2016). *S. stocksii* (Duthie) Gamble is an endangered species endemic to Southwest India (Byng *et al.,* 2015). The strong antimicrobial activity of the essential oils from *S. polyanthum*, *S. alternifolium*, *S. samarangense*, *S. caryophyllatum*, and *S. grande* has been documented previously (Kadir *et al.,* 2022). Although leaf extracts of *S. stocksii* and *S. densiflorum* have been screened for their preliminary antimicrobial activity (Eganathan *et al.,* 2012), no data are available regarding the composition and biological activity of essential oils from *S. stocksii*. In the present study, we explored the phytochemicals present in the leaves of *S. stocksii*. The essential oil in the leaves was isolated, and the leaves were extracted with different solvents. The essential oil was subjected to GC/MS analysis to identify its phytoconstituents. The antioxidant activity, total phenolic and flavonoid contents were estimated. The biosynthesis of silver nanoparticles was carried out by reducing Ag^+ ions using the ethanolic extract as a stabilizing and reducing agent. The essential oils, extracts, and biosynthesized AgNPs were tested for antimicrobial and antibiofilm activities, and some promising results were obtained.

Materials and methods

Collection of plant material and oil extraction

The plant species *Syzygium stocksii* (Duthie) Gamble was collected in September 2022 from Cherupuzha, Kasaragod, Kerala, India (latitude 12°16’22.1002” N, longitude 75°21’15.3277” E). The identification was

confirmed by a taxonomist, and voucher specimens were stored at the University College Herbarium, Thiruvananthapuram, Kerala, India, under accession number 0082. Fresh leaves of *S. stocksii* were collected and shade-dried for seven days before being pulverized into a coarse powder. Approximately 80 g of the powder was placed in a 1 L round-bottom flask, and hydrodistillation was conducted for 6 h to collect the oil.

GC/MS analysis of essential oil

The essential oil was analyzed using a Shimadzu Nexis GC-2030 linked to a QP-2020 NX mass spectrometer. 1 µL sample was injected in split mode at 240 °C. Helium was used as the carrier gas at a flow rate of 1.4 mL/min. The oven temperature ranged from 60 to 250 °C, and mass spectra were obtained in Electron Impact mode (70 eV). The constituents were identified using the MS library search.

Phytochemical analysis

Sequential extraction of 25 g of pulverized plant material was performed using hexane, ethyl acetate, and ethanol in a Soxhlet apparatus. The crude extracts were dried and dissolved in methanol for subsequent phytochemical analysis. The Folin-Ciocalteu method was used to determine the total phenolic content using gallic acid as standard and expressed in mg GAE/g of the extract. The $AlCl_3$ colorimetric assay was used to assess the total flavonoid content, using quercetin as standard and expressed in mg QE/g of the extract. Antioxidant activity was evaluated using the DPPH radical-scavenging assay. Extracts (1 mg/mL) and a standard (BHA) were mixed with DPPH solution and incubated. The absorbance was measured at 515 nm. Methanol served as the blank, and BHA was used as the positive control. The inhibition percentages and IC_{50} values were calculated.

Synthesis of silver nanoparticles

Dried ethanolic plant extract (0.5 g) was dissolved in 100 mL of distilled ethanol [SSE-NP] for the synthesis of nanoparticles. An aqueous $AgNO_3$ solution (1 mM, 5 mL) was heated to 80 °C for 5 min using a magnetic stirrer. Then, 2 mL of SSE-NP and one drop of 0.05 M NaOH were added, and the mixture was heated again at 80 °C until the solution turned golden yellow, indicating silver nanoparticle formation (Kolya *et al.,* 2015). SSE functioned as both a reducing and capping agent. The change from green to golden yellow was visually evident, and UV-Vis spectra showed surface plasmon resonance (SPR) at 425 nm, with variations in the concentration of $AgNO_3$ and reaction time. Phytochemicals, particularly amino acids, contribute to the reduction of Ag(I) to silver nanoparticles (Huo *et al.,* 2022).

Characterization of silver nanoparticles

The UV-Vis spectra of the synthesized AgNPs were measured in a 1 cm quartz cuvette using a Shimadzu UV-2450 (Japan) spectrophotometer. The morphology and size of AgNPs were studied using a transmission electron microscope (TEM) model JEOL-JEM-1010 (Japan), a 100 kV high contrast electron microscope with a magnification of up to 300K. The sample for the TEM study was made by depositing a drop of silver sol onto a carbon film mounted on a copper grid (3.05 mm diameter) and evaporating the solvent. The copper grid was carefully placed on the fully eucentric goniometer specimen stage for analysis. The FTIR spectrum of AgNPs was obtained using Shimadzu IR Prestige- 21 (Japan), with a scan range of 400-4000 cm^{-1}, at a resolution of 8 cm^{-1}, in which the potassium bromide (KBr) pellet technique was employed for spectral analysis.

Antimicrobial studies

The bacterial and fungal isolates were American Type Culture Collection (ATCC) strains: *Acinetobacter baumannii* (ATCC 5663), *Pseudomonas aeruginosa* (ATCC 9027), *Bacillus cereus* (ATCC 10876), and *Streptococcus mutans* (ATCC 25175), and the fungal species, *Candida albicans* (ATCC 90028), were purchased from NCIM Pune, India. Antimicrobial activity was assessed using the disc diffusion method. Bacteria were grown on Mueller–Hinton agar plates, and test samples were applied to discs. The plates were incubated at 37 °C. A concentration of 42 mg/mL of dried extract was used for the studies. A disc containing 46 µg of ciprofloxacin (CIP) was used as a positive control. The microtiter broth dilution method was used to estimate the minimum inhibitory concentration (MIC) of SSO, in accordance with the Clinical and Laboratory Standards Institute (CLSI) standards. Bacterial suspensions were mixed with serial dilutions of the oil, incubated overnight, and the MIC was visually determined as the lowest concentration that showed no growth.

Antibiofilm activity

The antibiofilm activities of various compounds were assessed using the crystal violet (CV) assay. Overnight cultures of *P. aeruginosa* (ATCC 9027) were diluted to ~1×10^6 CFU/mL and added (200 µL) to each well of sterile 96-well microtiter plates. Samples (10 µL) were introduced with a negative control of bacterial culture without samples. The plates were incubated statically for 24 hours at 37 °C. After incubation, biofilm quantification was performed as described with the technique (Mini *et al.,* 2023, Rani *et al.,* 2024). The results were enumerated using a Thermo Scientific Multiskan FC microplate reader (version 1.01.17). Biofilm generation without compounds was considered 100%, whereas the sterile medium control was 0%. Three biological replicates were performed, and the results were averaged.

Results and discussion

Yield and composition of essential oil

The essential oil from *S. stocksii* leaves (SSO) obtained by hydrodistillation yielded 0.13% (w/w). The yield was calculated according to reported method (Zhang *et al.,* 2015). GC/MS analysis of the oil (Table 1) revealed the

Table 1: Chemical composition of *Syzygium stocksii* essential oil

Peak	RT (min)	Compounds	%
1	6.690	β-Myrcene	0.71
2	8.020	(E)-β-Ocimene	12.60
3	8.522	(Z)-β-Ocimene	69.71
4	14.812	3-p-Menthen-7- al	0.77
5	18.304	*Cis*-p-Mentha-2,8-dien-1-ol	0.71
6	22.091	6,6-dimethyl-2-methylene-bicyclo [3,1,1] heptane	1.85
7	23.678	4,11,11-trimethyl-8-methylene-bicyclo [7,2,0] undec-4-ene	6.51
8	24.445	3,7,11-trimethyl-2,6,10-dodecatrien-1-ol	0.77
9	25.125	2,6,6,9-tetramethyl-1,4,8-cycloundecatriene	1.54
10	30.111	12- trimethyl-9-methylene-5-oxatricyclo[8.2.0.0]dodecane	4.85

presence of ten components, with the major components being (Z)-β-ocimene (69.71%) and (E)-β-ocimene (12.6%). This is the first phytochemical evaluation of *S. stocksii*, reporting the presence of ocimenes, which have been reported in other sources. The gas chromatogram (Supplementary Figure S1) and mass fragmentation patterns of the individual constituents (Supplementary Figure S2) are provided in the supplementary material.

Phytochemical analysis

The total phenolic content (TPC) was highest for the ethanol extract (SSE) at 53.01 mg GAE/g, while for the ethyl acetate extract (SSEA) and hexane extract (SSH), the TPC values were 8.82 mg GAE/g and 8.69 mg GAE/g, respectively, indicating a reasonably good overall phenolic content. The total flavonoid content (TFC) was highest in the hexane extract (117.52 mg QE/g), followed by ethyl acetate (109.67 mg QE/g) and ethanol (55.90 mg QE/g). Antioxidant activity, measured using the DPPH assay, showed IC_{50} values of 3199 ppm for ethyl acetate extract and 601.55 ppm for ethanol extract, in comparison with BHA at 50.17 ppm. However, the hexane extract and essential oil exhibited prooxidant activity. The standard calibration curves are provided in the Supplementary Figures S3 and S4).

UV-Vis, TEM & FT-IR analyses

Formation of the silver nanoparticles was visually evident from the colour change, i.e., green to golden yellow (Supplementary Figure S5). The UV-Vis spectra (Supplementary Figure S6) showed the appearance of surface plasmon resonance (SPR) centred around 425 nm. The TEM images (Supplementary Figure S7) show the characteristic identity of nanoparticles, which appear spherical and oval with particle sizes ranging from 10-20 nm. The FT-IR spectra of the ethanolic plant extract (Supplementary Figure S8) and green-synthesized AgNPs (Supplementary Figure S9) show similar peaks which indicate that the plant extract acts as a stabilizing agent as well as a capping agent. The green-synthesized Ag silver nanoparticles exhibited IR absorption peaks at 3500 cm^{-1} (O-H stretching), 2904.8 cm^{-1} (C-H stretching), 1635.64 cm^{-1} (C=O stretching), 1363.67 cm^{-1} (O-H in-plane bending), and 1126.43 cm^{-1} (C-O stretching). FT-IR spectrum of the plant extract displayed similar peaks, albeit with slight shifts, indicating the adsorption of biomolecules onto the surface of the AgNPs. This observation suggests that the biomolecules from the plant extract are involved in the capping and stabilization of the synthesized AgNPs, as described in the literature (Restrepo & Villa, 2021).

Antimicrobial studies

The antimicrobial assay results (Table 2), demonstrated that SSO exhibited high activity against both Gram-positive (*Bacillus cereus, Streptococcus mutans*) and Gram-negative pathogens (*Acinetobacter baumannii*, *Pseudomonas aeruginosa*), as well as the fungal pathogen *Candida albicans*. SSE exhibited moderate activity against the gram-positive bacteria *Bacillus cereus* and *Streptococcus mutans*, whereas Ag nanoparticles displayed moderate activity against all tested pathogens. Overall, SSO was the most effective antimicrobial agent tested. Owing to its exceptional activity, the minimum inhibitory concentration (MIC) of SSO was further evaluated. The MIC results (Supplementary Table S1) revealed that SSO was highly potent against *Streptococcus mutans* (0.326 mg) and *Acinetobacter baumannii* (1.305 mg), corroborating the findings of the disc diffusion assay. These results confirm that SSO is highly effective against both Gram-negative and Gram-positive bacteria, as well as fungal pathogens. Antimicrobial activity of the different samples against Gram-positive and Gram-negative bacterial strains, assessed using the disc diffusion method are included in the Supplementary Figures S10 and S11.

Antibiofilm activity

All samples, except SSE, significantly inhibited *P. aeruginosa* biofilm formation (Figure 1). Interestingly, the three different silver nanoparticle dispersions, SSNP1, SSNP2, and SSNP3, prepared using a solution (5 mg/mL) of the dried extract in ethanol (SSE-NP), inhibited biofilm formation by more than 98% despite their lack of antimicrobial properties. The plant extracts, SSH and SSEA, and SSE-NP inhibited biofilm formation by 68%, 75%, and 40%, respectively. Despite its high antimicrobial activity, SSO did not disrupt the total biofilm architecture of *P. aeruginosa* (18% inhibition).

Our results indicate that, similar to other species of the *Syzygium* genus, the essential oils of *S. stocksii* also possess potent antimicrobial properties. SSO is rich in β-ocimene, with *cis*-β-ocimene as the major component. The antimicrobial action of *S. stocksii* essential oil may be attributable (Mahdian *et al.,* 2017) to the presence of monoterpenes, β-myrcene, and β-ocimene, as evident from the GC-MS data. The essential oil exhibited potent *in vitro* antibacterial activity, particularly against Gram-positive bacteria.

The present investigation also found that the silver nanoparticles SSNP1, SSNP2, and SSNP3 inhibited more than 98% of the *P. aeruginosa* biofilm. Several studies have

Table 2: Zone of inhibition (mm) of samples against Gram positive, Gram negative bacterial and fungal strains

S. No.	Samples	Zone Size (mm)				
		Bacillus cereus	***Acinetobacter baumannii***	***Pseudomonas Aeruginosa***	***Streptococcus mutans***	***Candida Albicans***
1	SSO	12.92	8.92	14.14	21.77	23.06
2	Ciprofloxacin	13.03	17.92	13	22.44	23.3
3	SSE	10.72	7.37	7.23	12.83	8.68
4	Ethanol	7.446	8.62	9.15	7.43	10.66
5	SSH	NA	NA	NA	NA	NA
6	Hexane	NA	NA	NA	NA	NA
7	SSEA	7.19	7.68	8.52	6.21	6.62
8	Ethyl acetate	6.07	7.77	6.40	7.28	7.01
9	SSE-NP	9.44	11.48	9.34	10.30	8.30
10	SSNP1	NA	7.54	7.99	9.03	9.33
11	SSNP2	5.98	7.37	7.06	6.84	7.10
12	SSNP3	NA	6.85	7.04	7.01	8.69

SSO - *S. stocksii* leaf essential oil, SSE - *S. stocksii* leaf extract in ethanol, SSH - *S. stocksii* leaf extract in hexane, SSEA - *S. stocksii* leaf extract in ethyl acetate, SSE-NP - SSE solution (5 mg/mL) used for nanoparticle synthesis, SSNP1, SSNP2 and SSNP3 - Silver nanoparticles synthesized from SSE-NP under different conditions, NA - No Activity

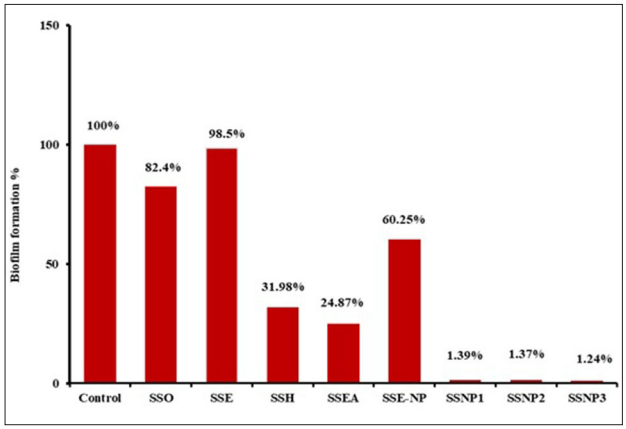

Figure 1: CV assay for 24-hour biofilm quantification showing the percentage of bacterial biofilm formation in the presence of samples, SSO, SSE, SSH, SSEA, SSE-NP, SSNP1, SSNP2, and SSNP3

demonstrated that AgNPs are effective against planktonic cells and bacterial biofilms. The mechanism by which AgNPs disrupt biofilms is not well understood; however, research indicates that biofilm inhibition may be due to a change in bacterial metabolism induced by nanoparticles (Wang *et al.,* 2017). Based on our observations of the exceptional anti-biofilm activity of the nanoparticles, silver nanoparticle-based antibiofilm coatings can be expected to have potential applications in the manufacture of medical implants, surgical tools, and other healthcare materials to eliminate biofilm formation and control microbial infections to a great extent. To fully understand the therapeutic potential of this underexplored *Syzygium* species, additional pharmacological investigations into its medicinal properties are warranted. Our investigations highlight the need for detailed preclinical and clinical investigations to evaluate the drug development potential of essential oils and extracts from *S. stocksii*.

Conclusions

The phytochemical and biological activity of *S. stocksii* leaves were examined in this study. GC/MS analysis revealed the presence of β-ocimenes (E and Z). We evaluated the antioxidant activity and calculated the total flavonoid and phenolic concentrations, obtaining reasonably good results. The green production of silver nanoparticles with a size of 10-50 nm was successfully accomplished using an ethanolic extract. *A. baumannii* and *S. mutans* showed the highest sensitivity to the essential oil, with minimum inhibitory concentrations (MIC) of 1.305 and 0.326 mg, respectively, according to antimicrobial investigations. More importantly, the antibiofilm activity of the AgNPs against *P. aeruginosa* by more than 98% was exceptional, a promising observation for further development for applications such as antimicrobial coatings.

Acknowledgments

The authors thank Dr. K. B. Rameshkumar, CIF, KSCSTE- JNTBGRI, Thiruvananthapuram, for GC-MS analysis and Dr. G. S. Vinod Kumar, RGCB, Thiruvananthapuram, for TEM analysis. The authors are thankful for the facilities provided by the Government College for Women, Thiruvananthapuram. The Kerala State Council for Science, Technology, and Environment (KSCSTE) is acknowledged for the Junior Research Fellowship awarded to B. S. Devika. The Junior Research Fellowship awarded to J. Devi by the University Grants Commission (UGC) is also acknowledged. The financial support by the Government of Kerala, India, under the PLEASE programme and the research funding under Consolidation of University Research for Innovation and Excellence in Women Universities (CURIE), DST, New Delhi, are also acknowledged.

Author contributions

B. S. Devika: sample collection, phytochemical investigations, nanoparticle preparation, activity studies and writing the original draft. J. Devi: performing antimicrobial studies and microbial film growth inhibition. P. Biju: taxonomical evaluation and supervision of the phytochemical evaluation. Praveen Kumar: formal validation and writing of biological activity studies. P. S. Hema: supervision of the chromatographic analysis and guidance on phytochemical studies. G. Ajayakumar: conceptualization of the work, overall supervision, review & editing. All authors approved the final manuscript.

References

Ahmad, B., Baider, C., Bernardini, B., Biffin, E., Brambach, F., Burslem, D., Byng, J. W., Christenhusz, M., Florens, F. B. V.,

Lucas, E., Ray, A., Ray, R., Smets, E., Snow, N., Strijk, J. S., Wilson, P. G., & Syzygium Working Group. (2016). *Syzygium* (Myrtaceae): Monographing a taxonomic giant via 22 coordinated regional revisions. *PeerJ Preprints, 4*, e1930v1. https://doi.org/10.7287/peerj.preprints.1930v1

Amorati, R., Foti, M. C., & Valgimigli, L. (2013). Antioxidant activity of essential oils. *Journal of Agricultural and Food Chemistry, 61*(46), 10835-10847. https://doi.org/10.1021/jf403496k

Antimicrobial Resistance Collaborators. (2022). Global burden of bacterial antimicrobial resistance in 2019: A systematic analysis. *The Lancet, 399*(10325), 629-655. https://doi.org/10.1016/S0140-6736(21)02724-0

Babaei, F., Nassiri-Asl, M., & Hosseinzadeh, H. (2020). Curcumin (a constituent of turmeric): New treatment option against COVID-19. *Food Science & Nutrition, 8*(10), 521-532. https://doi.org/10.1002/fsn3.1858

Byng, J., Wilson, P., & Snow, N. (2015). Typifications and nomenclatural notes on Indian Myrtaceae. *Phytotaxa, 217*(2), 101-116. https://doi.org/10.11646/phytotaxa.217.2.1

Cascioferro, S., Carbone, D., Parrino, B., Pecoraro, C., Giovannetti, E., Cirrincione, G., & Diana, P. (2021). Therapeutic strategies to counteract antibiotic resistance in MRSA biofilm-associated infections. *ChemMedChem, 16*(1), 65-80. https://doi.org/10.1002/cmdc.202000677

Eganathan, P., Saranya, J., Sujanapal, P., & Parida, A. (2012). Antimicrobial activity of *Syzygium stocksii* (Duthie) Gamble and *Syzygium densiflorum* Wall. ex Wt. & Arn. leaves. *Journal of Biologically Active Products from Nature, 2*(6), 360-364. https://doi.org/10.1080/22311866.2012.10719144

Huo, C., Hao, Z., Yuan, C., Chen, Y., & Liu, J. (2022). Probing the phytosynthesis mechanism of gold and silver nanoparticles by sequential separation of plant extract and molecular characterization with ultra-high-resolution mass spectrometry. *ACS Sustainable Chemistry & Engineering, 10*(12), 3829-3838. https://doi.org/10.1021/acssuschemeng.1c07021

Kadir, N. H. A., Salleh, W. M. N. H. W., & Ghani, N. A. (2022). A systematic review on essential oils and biological activities of the genus *Syzygium* (Myrtaceae). *Rivista Italiana delle Sostanze Grasse, 99*(3), 165-178.

Kolya, H., Maiti, P., Pandey, A., & Tripathy, T. (2015). Green synthesis of silver nanoparticles with antimicrobial and azo dye (Congo red) degradation properties using *Amaranthus gangeticus* Linn leaf extract. *Journal of Analytical Science and Technology, 6*, 33. https://doi.org/10.1186/s40543-015-0074-1

Lewis, K., & Ausubel, F. M. (2006). Prospects for plant-derived antibacterials. *Nature Biotechnology, 24*, 1504-1507. https://doi.org/10.1038/nbt1206-1504

Mahdian, F., Mahboubi, M., Rahimi, E., & Shad, M. M. (2017). Chemical composition, antimicrobial and antioxidant activities of *Echinophora platyloba* essential oil. *Infectio, 21*(3), 153-158. https://doi.org/10.22354/in.v21i3.675

Mini, M., Jayakumar, D., & Kumar, P. (2023). *In-silico* and *in-vitro* assessment of the antibiofilm potential of azo dye, carmoisine against *Pseudomonas aeruginosa*. *Journal of Biomolecular Structure and Dynamics, 42*(13), 6700-6710. https://doi.org/10.1080/07391102.2023.2237579

Qayyum, S., & Khan, A. U. (2016). Nanoparticles vs. biofilms: A battle against another paradigm of antibiotic resistance. *MedChemComm, 7*(8), 1479-1498. https://doi.org/10.1039/C6MD00124F

Rani, A., Asha, S., Mini, M., Rajan, P. P., Tomy, M., Jose, A., Xavier, T. S., & Kumar, P. (2024). Exploring the antibacterial and antibiofilm potential of copper oxide nanoparticles biosynthesized using *Centratherum punctatum* leaf extract. *South African Journal of Botany, 164*, 1-8. https://doi.org/10.1016/j.sajb.2023.11.020

Restrepo, C. V., & Villa, C. C. (2021). Synthesis of silver nanoparticles, influence of capping agents, and dependence on size and shape: A review. *Environmental Nanotechnology, Monitoring & Management, 15*, 100428. https://doi.org/10.1016/j.enmm.2021.100428

Siddiqui, M. W., & Prasad, K. (2016). *Plant secondary metabolites, volume one: Biological and therapeutic significance.* Apple Academic Press. https://doi.org/10.1201/9781315366326

Simões, M., Bennett, R. N., & Rosa, E. A. S. (2009). Understanding antimicrobial activities of phytochemicals against multidrug resistant bacteria and biofilms. *Natural Product Reports, 26*(6), 746-757. https://doi.org/10.1039/b821648g

Slavin, Y. N., Asnis, J., Häfeli, U. O., & Bach, H. (2017). Metal nanoparticles: Understanding the mechanisms behind antibacterial activity. *Journal of Nanobiotechnology, 15*, 65. https://doi.org/10.1186/s12951-017-0308-z

Wang, L. L., Hu, C., & Shao, L. Q. (2017). The antimicrobial activity of nanoparticles: Present situation and prospects for the future. *International Journal of Nanomedicine, 12*, 1227-1249. https://doi.org/10.2147/IJN.S121956

Zhang, D.-Y., Yao, X.-H., Duan, M.-H., Wei, F.-Y., Wu, G., & Li, L. (2015). Variation in essential oil content and antioxidant activity of *Lonicera* species at different sites in China. *Industrial Crops and Products, 77*, 772-779. https://doi.org/10.1016/j.indcrop.2015.09.048

Supplementary materials

GC/MS analysis

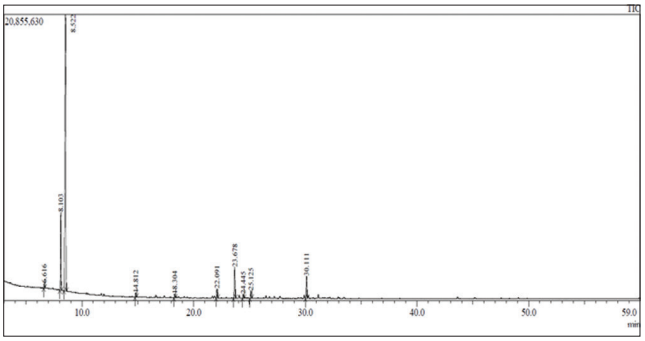

Supplementary Figure S1: Gas Chromatogram of the essential oil derived from the leaves of *S. stocksii*

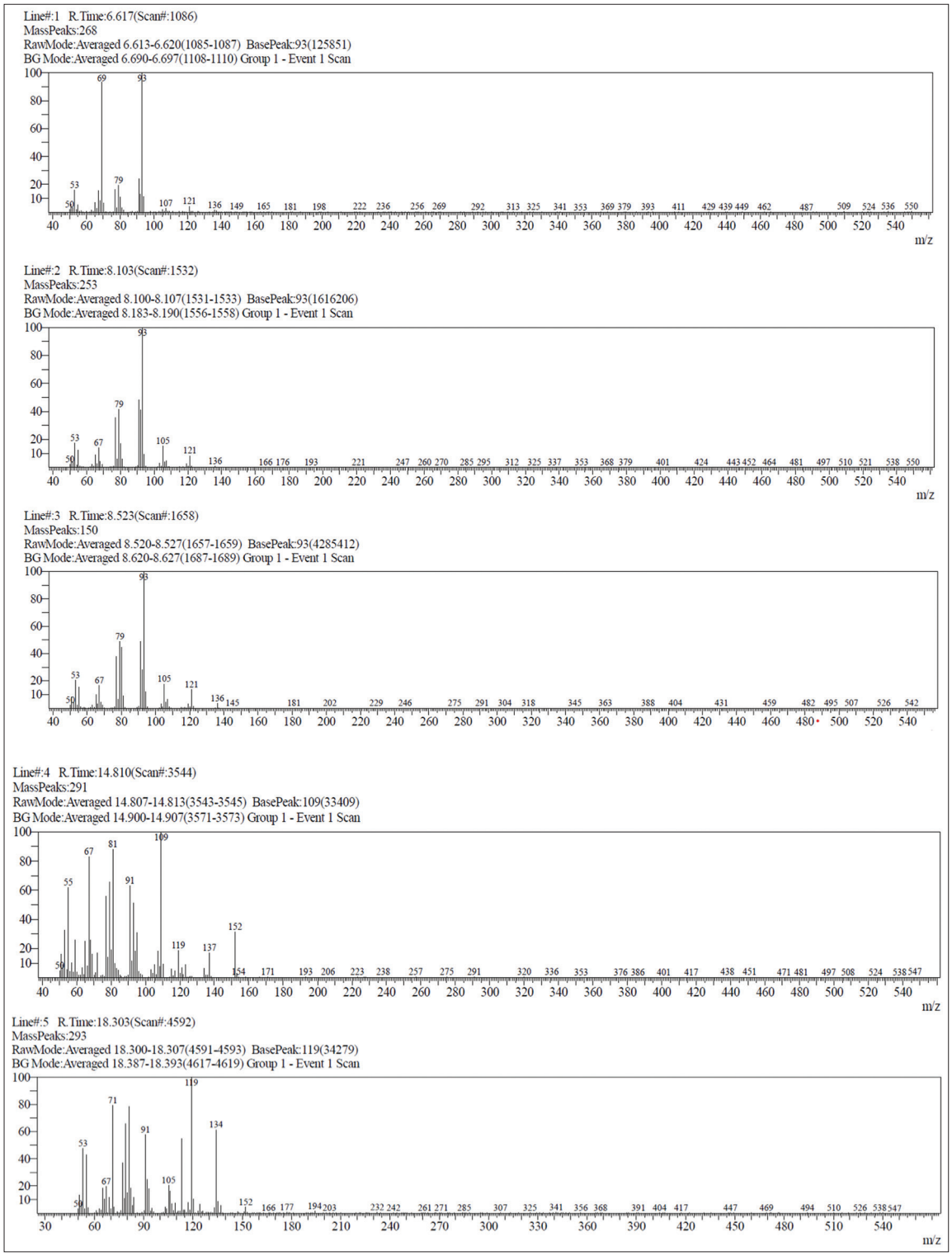

Supplementary Figure S2: Mass fragmentation patterns (*Contd*)

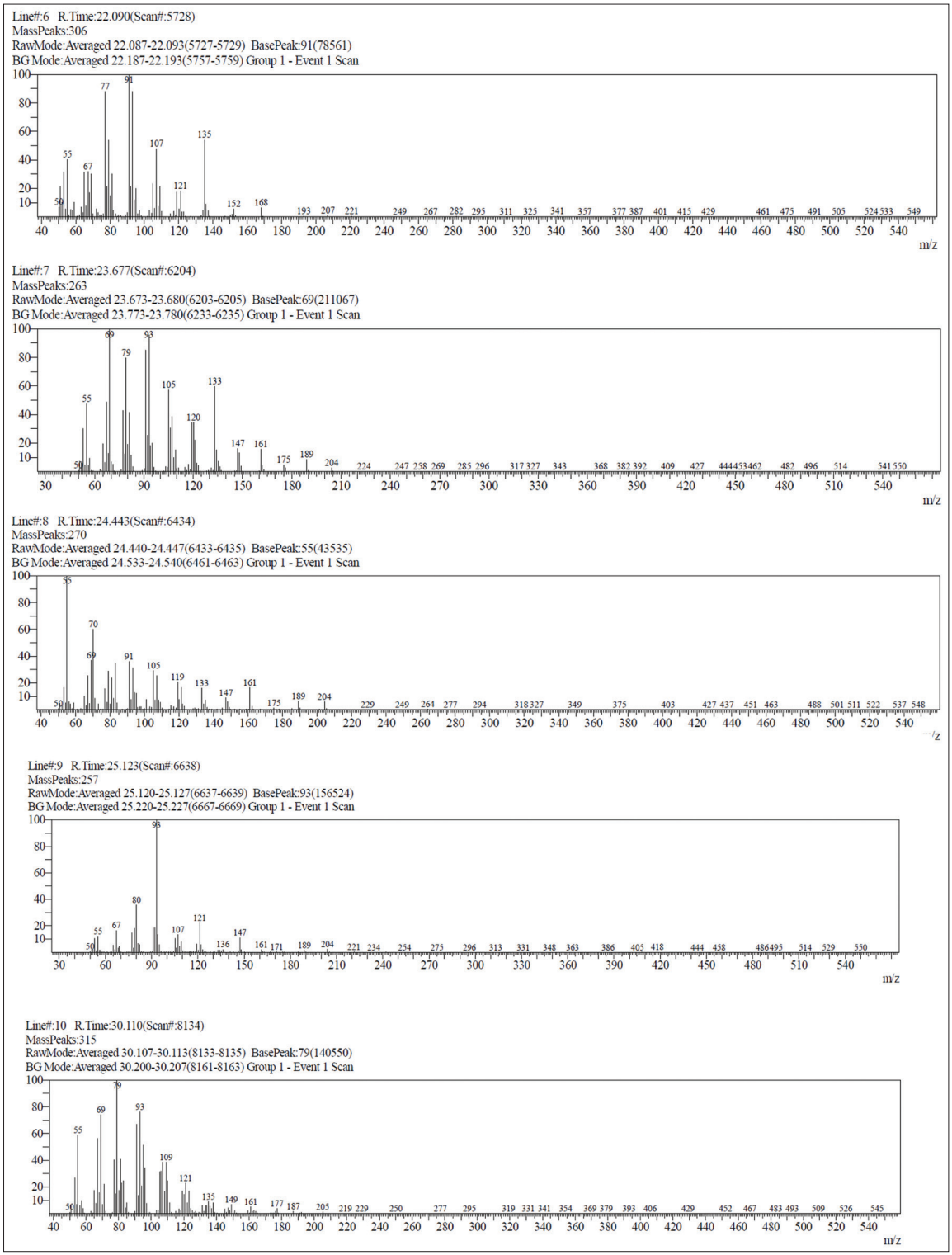

Supplementary Figure S2: (*Continued*)

Analysis of phenolic and flavonoid contents

The standard calibration curve of gallic acid, obtained by plotting the absorbance against the respective concentrations, is as follows:

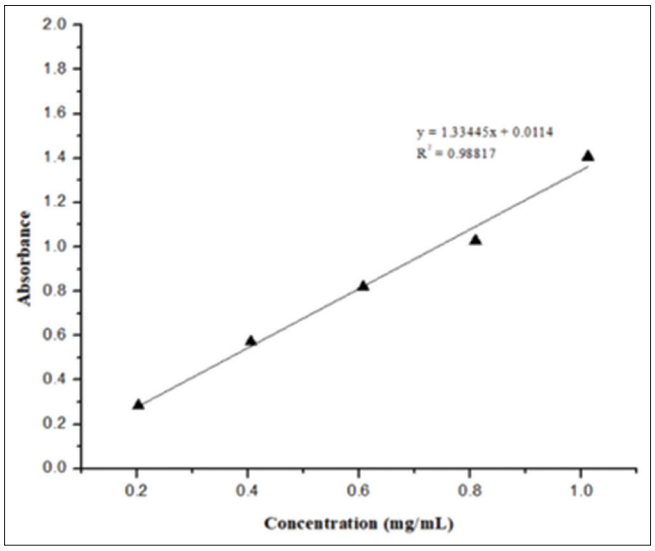

Supplementary Figure S3: Standard calibration curve of gallic acid

The standard calibration curve of quercetin, obtained by plotting the absorbance against the respective concentrations, is as follows:

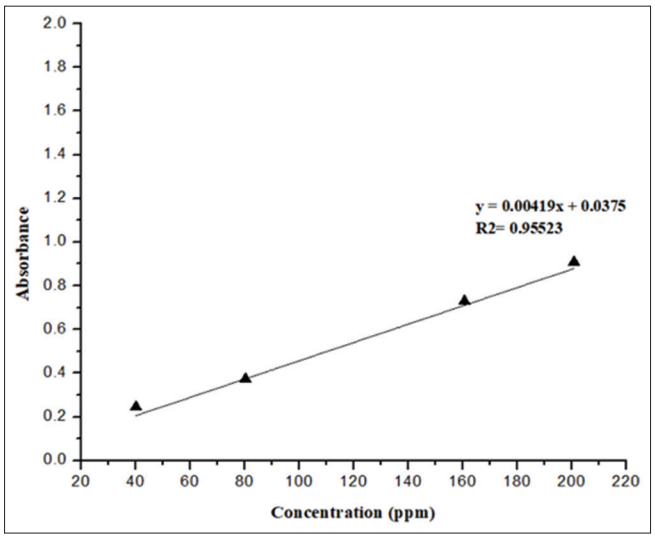

Supplementary Figure S4: Standard calibration curve of quercetin

Green synthesis of silver nanoparticles and characterization

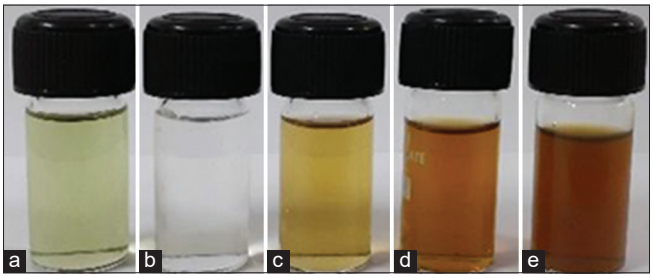

Supplementary Figure S5: Photographs of a) Ethanolic extract b) 1 mM silver nitrate solution and AgNPs with SPR peak at c) 416 nm d) 422 nm and e) 434 nm

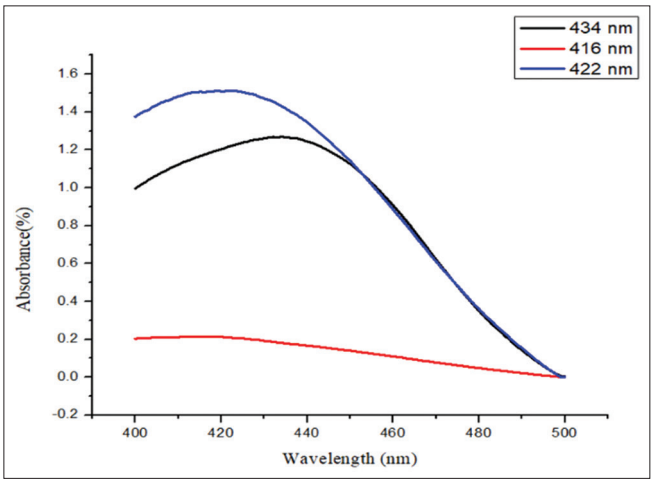

Supplementary Figure S6: UV- Visible spectra of AgNPs

Transmission Electron Microscopy (TEM) studies

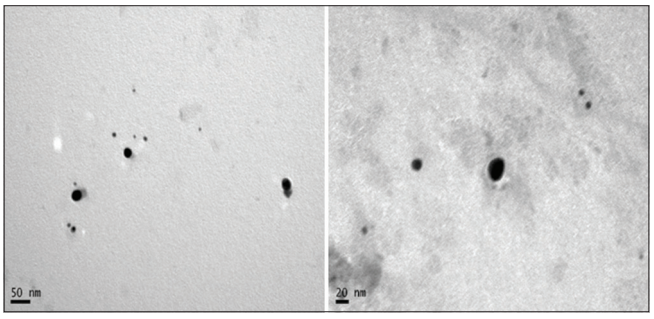

Supplementary Figure S7: TEM images of green synthesized AgNPs

FT-IR studies

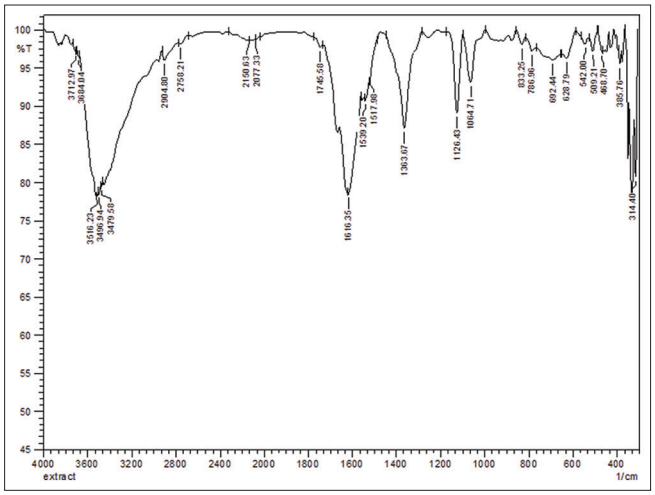

Supplementary Figure S8: FTIR Spectrum of the plant extract

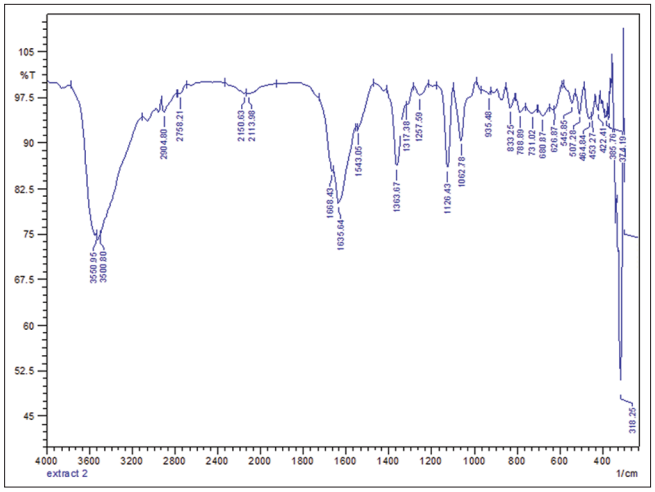

Supplementary Figure S9: FTIR spectrum of AgNPs

Minimum Inhibitory Concentration (MIC)

Supplementary Table S1: Minimum Inhibitory Concentration (MIC) of SSO against gram positive and gram-negative bacterial strains

Bacterial Sp.	MIC (mg)
Bacillus cereus	2.61
Acinetobacter baumannii	1.305
Pseudomonas aeruginosa	5.22
Streptococcus mutans	0.326

Antimicrobial studies

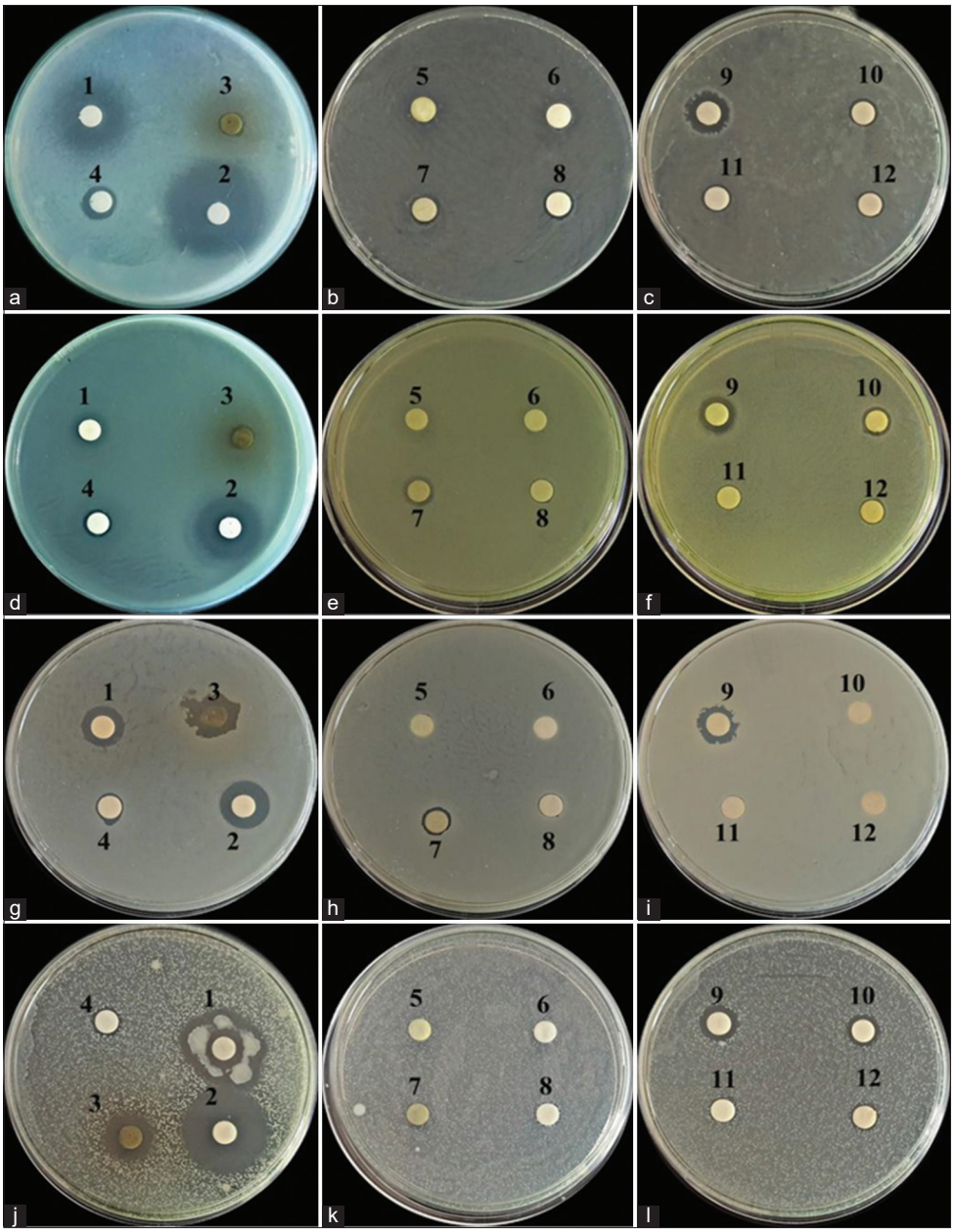

Supplementary Figure S10: Antimicrobial assay of samples against Gram-positive Gram-negative bacterial strains. Plates a, b, c) represent *Acinetobacter baumannii*, d, e, f) represent *Pseudomonas aeruginosa*, g, h, i) represent *Bacillus cereus*, and j, k, and l) represent *Streptococcus mutans*. The numbers 1, 2, 3, 4, 5, 6, 7, 8, 9, 10, 11, and 12 represent discs containing SSO, CIP, SSE, Ethanol, SSH, Hexane, SSEA, Ethyl acetate, SSE, SSNP1, SSNP2, and SSNP3, respectively

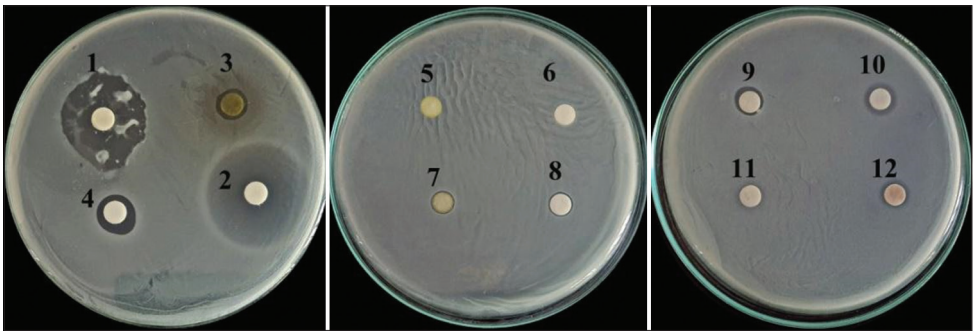

Supplementary Figure S11: Antimicrobial assay of samples against the fungal pathogen *Candida albicans*. The numbers 1, 2, 3, 4, 5, 6, 7, 8, 9, 10, 11, and 12 represent discs containing SSO, CIP, SSE, Ethanol, SSH, Hexane, SSEA, Ethyl acetate, SSE, SSNP1, SSNP2, and SSNP3, respectively